Impact of the User Charging Practice on the Battery Aging in an Electric Vehicle

Alla Ndiaye, Ronan German, Alain Bouscayrol, M. Gaetani-Liseo, P. Venet, Elodie Castex

Impact of the User Charging Practice on the Battery Aging in an Electric Vehicle

A. Ndiaye, R. German, A. Bouscayrol, M. Gaetani-Liseo, P. Venet, E. Castex

Abstract— This paper studies how the user charging practice affects battery degradation over time. To achieve this objective, a system oriented simplified aging model based on the literature is proposed. The differential calculation of the capacity loss is used for infinitesimal variations. The model inputs are the battery state of charge, the battery temperature and the cumulative number of full equivalent cycles. The output is the battery state of health. This model is identified and validated with experimental aging tests from the Renault Zoe 41kWh battery manufacturer. The battery model (electro-thermal and aging) interconnects with the vehicle traction model complete the system model. The battery electro-thermal and traction models are also validated with measurements on the studied vehicle. The Energetic Macroscopic Representation (EMR) formalism organizes in a unified way the interconnections of all the sub-system models. The impact of the charging interval and SoC on the battery aging is then studied. Five charging scenarios are studied by simulation while keeping the driving phases and the charging current the same. In these conditions, the average SoC is the main contributor for the battery aging. Compared to daily charge of the EV, a charge every 4 days extends the time to reach 80% of state of health by 36 % due to lower average SoC. The daily driving distance is fixed for every studied scenario.

***Index Terms*— Electric vehicle; energetic macroscopic representation; Li-ion battery; charging; aging.**

I. Introduction

Electric Vehicles (EVs) [1] [2] reduce greenhouse gases (GHG) emissions due to transportation and limit global warming [3]. However, the GHG emissions due to EVs (also referred as Battery Electric Vehicles in some other publications BEVs [4]) production are high due to lithium mining, and the well to tank emissions are dependent on the way the electricity is produced [5]. Nevertheless, there is a global life cycle assessment gain in term of CO_2 compared to a classical thermal vehicle [6].

For EVs, the main energy source is a lithium-ion battery. The main technology currently used (for positive electrode) is the Nickel Manganese Cobalt (NMC) one [7]. In 2022, 75% of the battery demand for the electrified vehicles (EV or hybrid vehicles) is NMC [3]. Typical EVs have a driving range from 200 km to 400 km and a long charging time (up to 12 hours) [8].

As batteries represent a major cost of EVs, aging of batteries has been an important research topic for EVs. Batteries are complex storage systems based on electrochemistry. They are affected by many parameters such as temperature [9], State of Charge, cumulated cycles, etc. This results in battery aging over time [10].

Submitted 29 April 2023, revised 10 October 2023, accepted 16 January 2024.

A. Ndiaye, R. German and A. Bouscayrol are with Univ. Lille, Centrale Lille, Arts et Métiers Paris Tech, HEI, EA 2697 – L2EP - Laboratoire d'Electrotechnique et d'Electronique de Puissance, F-59000 Lille, France and -the French network on HEVS and EVS, MEGEVH, France (email: givenname.name@univ-lille.fr).

E. Castex is with the TVES of Lille, University of Lille, 59000 Lille, France (e-mail: elodie.castex@univ-lille.fr).

M. Gaetani-Liseo and P. Venet are with Univ Lyon, Université Claude Bernard Lyon 1, Ecole Centrale de Lyon, INSA Lyon, CNRS, Ampère, F-69100 Villeurbanne, France (email: givenname.name@univ-lyon1.fr).

As stated in a literature review [11], different types of battery aging models exist. Electrochemical models are used for analysis, but they are difficult to connect to other subsystems because of the specific variables they use [12]. Empirical black box models need large datasets for identification [13]. The semi empirical models are the most used for its advantage in identification and interconnection. This is the type of model used in this paper.

One of the aging indicators is the capacity decrease over time [14]. Aging of the battery is influenced by driving, charging [15] and parking (also called calendar ageing [16]). Charging can be managed to slow down battery aging. For example, varying charging power is studied to optimize the charging duration [17] or the battery lifespan [18], [19], [20]. Some experimental aging tests based on SoC [21], [22] have shown that the degradation of battery cells is faster when the SoC is higher.

The objective of this paper is to study the impact of the user charging practice (the time interval between battery charges or the SoC at which the user starts charging) on battery aging in an EV.

In the literature, various battery aging models have been developed with some missing aspects to be fully applied in the EV system. For example, in [23] an aging model is developed for large temperature span (0-55°C), but it is not in dynamic interaction with a traction model of an EV. In [24], an aging model is proposed considering the temperature and voltage but not the energy exchange through full equivalent cycle counting. In [25] an aging model is interconnected with a traction model. In this model the effect of cycles on aging is multiplicative. That means the capacity degradation is null if there is no exchange of energy. As a consequence, aging during parking mode cannot be considered in [25].

The scientific novelty of our paper is to integrate the battery model with aging as a sub-system of an EV. This model is considering all modes (parking, driving and charging). The system philosophy is based on the interconnection between different subsystems.

As a consequence, a simplified semi empirical aging model is proposed here. It is derived from classical models of the literature. The SoC and T dependence come from [25] and the energy exchange effect cumulative effect comes from [21] and [23]. It is composed of an electrical part, a thermal part and an aging part. This model is interconnected with the traction model of EV. Usage scenarios are considered from the perspective of the drivers: commuting trip, parking time and charging.

For this integration, the Energetic Macroscopic Representation (EMR) formalism is used [26]. The EMR is a graphical representation using power flows between different pictograms (see Appendix A). Moreover, the inputs and outputs of different pictograms are imposed by the integral causality (outputs are delayed compared to inputs). For these reasons, interconnection of multi-physical subsystems is facilitated and organised in a systematic way. The global model is thus organized in this unified way to enable the right interaction between subsystems models.

In section II, the global model is proposed and the parameters are identified from a set of experiments coming from an EV NMC cell manufacturer. Validations of each sub-system with experimental results are performed. In section III, different scenarios are presented and studied. Battery aging is simulated and compared for 10 years, which corresponds to a classical vehicle ownership duration. Literature and industrial policy recommend to change an EV battery when the State of Health (SoH) reaches 80% to 70 % [27][28][29] where the SoH is defined as the ratio between the actual capacity versus the initial capacity at the battery Beginning of Life (BoL). A comparative study is performed to estimate the time to reach 80% SoH in this paper.

II. Modelling of the Battery and the Vehicle

A. Battery aging model presentation

The main aging factors associated to batteries are well identified in the literature [30]:

- the state of Charge (*SoC* in %),
- the temperature of the battery (T_{Bat} in K),
- the time (in days),
- the number of cumulated Full Equivalent Cycles (N_{FEC}) since the battery production. One FEC corresponds to a full charge and discharge.

A system-oriented simplified aging model with two parts (1) is developed from existing aging models of the literature [23], [31], [32]. A set of experimental results [33] is used for identification. They correspond to the cell (63 Ah, NMC technology) used in the Renault Zoe 41 kWh. They correspond to mild to hot conditions). As a consequence, the extracted model is limited to normal to hot conditions. For the first part of the model, three classical stress factors are considered: SoC, temperature and time. To build the corresponding part of the equation the following assumptions are used. The aging SoC dependency is considered to be linear as in [31]. A classic Arrhenius law can be used to describe the impact of the temperature on aging as in [23]. The time dependence can be composed of a fractional exponent z (between 0 and 1) as in [32]. This first part represents the aging due to the SoC and temperature of the battery at any time. A second part is added to consider the number of FEC for a given charging/discharging current. It represents the aging due to the exchange of energy when battery is running. Aging is the sum of these two parts [34]. That means that the two parts are cumulative and occur at the same time. It is validated in the next sections with experimental results.

C_{loss} expressed in % here. As the input variables (*SoC*, T_{Bat} and N_{FEC}) are varying with time during an EV use, an approach based on a differential form is proposed in this paper such as [21] by adding the impact of N_{FEC} to consider energy exchange. The expression of the capacity loss variation for an infinitesimal time dt is given below.

$$dC_{loss_{t\to t+dt}} = d\left[(A + B.SoC)e^{\frac{-Ea}{k_B T_{Bat}}}.t^z + k_{FEC}.N_{FEC}\right] \quad (1)$$

where E_a is the energy of activation (eV), k_B is the Boltzmann constant (eV) and k_{FEC} is the capacity loss for each full equivalent cycle (% FEC^{-1}). Contrary to [23], k_{FEC} is taken as a constant. This simplification has to be verified with experimental results. To consider the history of the battery, the cumulated capacity loss is obtained by integrations.

$$C_{loss_{0\to t}} = \int_0^t dC_{loss} \quad (2)$$

The differential is expressed with partial derivatives and variations of each model variables (during $t \to t+dt$). Contrary to [21] and [31], the total differential is used here, instead of the partial differential in function of time.

$$dC_{loss_{(t\to t+dt)}} = \frac{\partial C_{loss}}{\partial SoC}dSoC + \frac{\partial C_{loss}}{\partial T_{Bat}}dT_{Bat} + \frac{\partial C_{loss}}{\partial t}dt + \frac{\partial C_{loss}}{\partial FEC}dFEC \quad (3)$$

The analytical expressions of partial derivatives are deduced from (1), they are given below.

$$\begin{cases} \frac{\partial C_{loss}}{\partial SoC} = B.e^{\frac{-E_a}{k_B.T_{Bat}}}.t^z \\ \frac{\partial C_{loss}}{\partial T_{Bat}} = \frac{E_a}{k_B.{T_{Bat}}^2}.e^{\frac{-E_a}{k_B.T_{Bat}}}(A + B.SoC)t^z \\ \frac{\partial C_{loss}}{\partial t} = (A + B\,SoC)e^{\frac{-E_a}{k_B.T_{Bat}}}\,z\,t^{z-1} \\ \frac{\partial C_{loss}}{\partial FEC} = k_{FEC} \end{cases} \quad (4)$$

A discretization of the law (1) is given with Δt the time step of the aging model (100 s) (5). This is infinitesimal compared to the aging time (~10 years).

$$\Delta C_{loss_{t\to t+\Delta t}} = \frac{\partial C_{loss}}{\partial SoC}\Delta SoC + \frac{\partial C_{loss}}{\partial T_{Bat}}\Delta T_{Bat} + \frac{\partial C_{loss}}{\partial t}\Delta t + \frac{\partial C_{loss}}{\partial FEC}\Delta FEC \quad (5)$$

The cumulated aging (2) is also discretized with a sum.

$$\Delta C_{loss_{0\to n\Delta t}} = \sum_{i=1}^{n} \Delta C_{loss_i} \quad (6)$$

As a consequence, the expression of the current degraded capacity of the battery (%) can be expressed as follows. In the battery this value is called the SoH.

$$SoH(t = n\Delta t) = 100 - \sum_{i=1}^{n} \Delta C_{loss_i} \quad (7)$$

where 100% is the normalized value of the fresh capacity. The value of the degraded capacity is one of the most important variables for EV simulation (for example for driving range estimation). It is smoothed with a low pass filter. The SoH is the output of the aging model.

B. SoC and temperature dependence identification

Experimental aging results from the literature are available in [33]. They correspond to the battery cells used in the 41 kWh Renault Zoe (LG Chem NMC 63 Ah). As any aging battery test, the test time (300 days) is much shorter than the battery lifetime (~10 years). They are used to extract the parameters of the capacity evolution with time. In the next sections, the extracted

models will be used for simulation during several years. The hypothesis is that the SoH behaviour stays the same until 70% of SoH. For the cells we are studying aging behaviour is steady until that limit [33]. This indicates that the ageing mechanism is dominated by the surface electrolyte interface growth and can be described by a single equation [35]. As a consequence, using shorter time aging test for identification is possible. The experimental results presented in Fig. 1 correspond to calendar aging. Calendar aging is particular kind of accelerated aging test where:

- no current is implied (ΔFEC=0, ΔSoC=0),
- the temperature is maintained constant with a thermal chamber (ΔT_{Bat}=0).

Consequently, the expression presented in (1) can be simplified as it is described as follows.

$$C_{loss}(t) = (A + B\,SoC)e^{\frac{-E_a}{k.T}}\ t^z \qquad (8)$$

This experimental test is used to identify the parameters *A*, *B*, E_a and *z*. A global data fitting is performed between the proposed model and experimental results to obtain the model parameters presented below.

Table 1 Identified aging law parameters due to SoC, T_{Bat} and t.

Parameter	Name	Value	Unit
Aging order	*z*	0.56	---
Aging SoC constant	*A*	942	% d^{-z}
Aging SoC dependence	*B*	68.3	% d^{-z} $(\%_{SoC})^{-1}$
Arrhenius activation energy	E_a	0.26	*eV*
Boltzmann constant	k_B	8,62.10^{-5}	*eV* K^{-1}

The capacity are normalized in % and d refer to days. Different indicators are used to quantify the accuracy of the model. First, in *Fig. 1* the determination coefficient (R^2) is added. Its value is independent whether C_{Loss} or *SoH* is represented.

$$R^2 = 1 - \frac{\sum\left(SoH_{Exp} - SoH_{Model}\right)^2}{\sum\left(SoH_{Exp} - \overline{SoH_{Exp}}\right)^2} \qquad (9)$$

where SoH_{Exp} is the experimental State of Health, SoH_{Model} is the predicted SoH and $\overline{SoH_{Exp}}$ is the average value of the experimental SoH. R^2 is better when SoC is high (0.99) than when aging constraints are low (~0.8). The relative errors are presented in Fig. 2. The average value of the relative error is 0.23 % for SoH.

This part of the aging model has been identified for a large span of SoC (5% to 90%) and of temperature (25°C to 45°C). This covers the majority of an EV use case in mild to hot weather conditions.

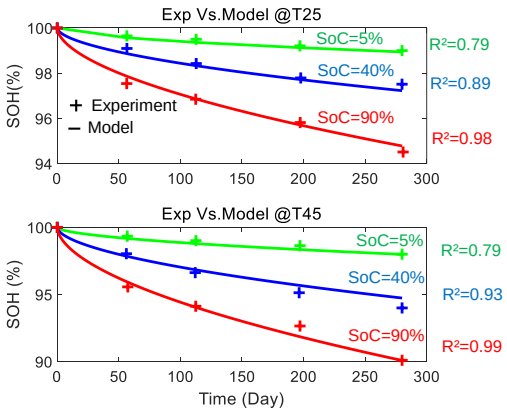

Fig. 1 Identification with experimental calendar aging results

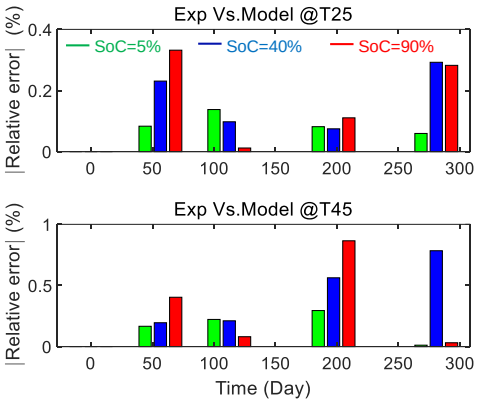

Fig. 2 Relative error on capacity for calendar aging

C. k_{FEC} identification

Experimental aging tests have been conducted with cycles (charging and discharging) by the battery cell manufacturer. In these experiments:

- current is running ($\Delta FEC \neq 0$, $\Delta SoC \neq 0$, $\Delta T_{Bat} \neq 0$),
- the ambient temperature is maintained constant with a thermal chamber.

Two ambient temperatures have been tested (25°C and 45°C). The cell SoC (Fig. 3.a) and the self-heating during a cycle (Fig. 3.b) are estimated from the manufacturer test procedure description given below [33].

- Charging: 21.6 A until U_{Cell} = 4.05 V then 13.0 A until U_{Cell} = 4.16 V.
- Constant voltage: 4.16 V until current reaches 3.2 A.
- Discharge: 32.5 A until U_{Cell} = 2.5V.

As the SoC goes from 0% to 100 % and back to 0%, a test cycle corresponds to a Full Equivalent Cycle (FEC). One FEC takes around 7 hours to be achieved. The experimental results of the manufacturer (Fig. 4) are used for k_{FEC} identification by data fitting, considering the other parameters of the aging model identified in Table 1.

The general model presented in (1) is used. The aging model is simulated with a fixed step size of 100 s (5)-(6).

The extracted k_{FEC} value is 98.0 10^{-3} % FEC^{-1}. The R^2 coefficient is calculated and presented in Fig. 4. The best value is 0.91 and the lower one is 0.82. The relative error on *C* is given for each point in Fig. 5.

The proposed model is close to the experimental SoH results (Fig. 4) It allows us to combine the effect of varying SoC, temperature and FEC with 2.20 % average relative error on the SoH.

The model has been identified for mild to hot temperatures (25°C to 45 °C) from experimental test of a manufacturer. As a consequence, the proposed battery aging model is restricted to these orders of temperature to have the announced accuracy. Studying cold temperatures would need other tests.

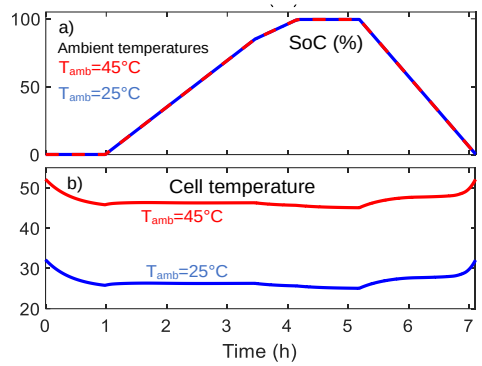

Fig. 3 SoC Estimated SoC a) and temperature b) evolution for an FEC

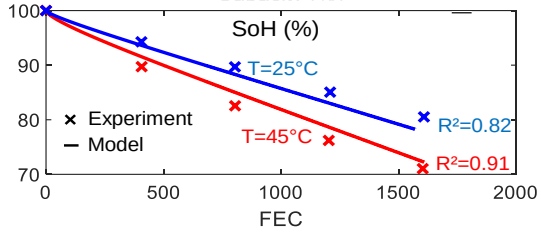

Fig. 4 Identification with accumulated FEC

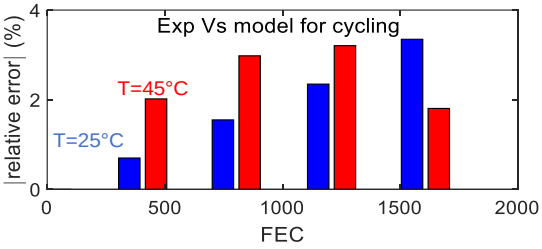

Fig. 5 Relative error on capacity as a function of the FEC

D. Aging model validation

To validate the aging model another aging test from the same document has been used [33]. It has not been used for identification. It is based on the cycle presented in Fig. 3a except that the charging phase at C/3 is replaced by a constant power at 43 kW which corresponds to a fast DC charge (Fig. 6). The coefficient of determination is 0.89 and the average relative error on SoH is 2.24 % (Fig. 7).

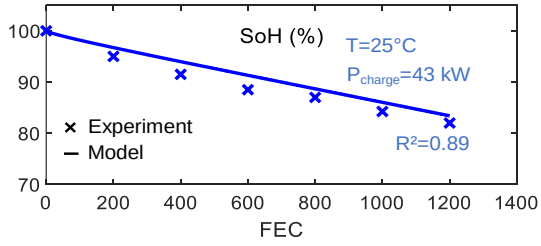

Fig. 6 Validation of the aging model with a fast recharge cycle

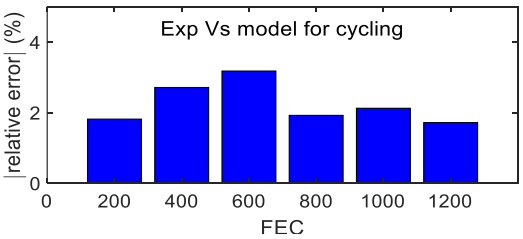

Fig. 7 Relative error for capacity with a fast recharge cycle

E. Simplified Battery Electro-Thermal model

The battery of the studied vehicle is composed of the cells presented before. The cells are assumed to be the same and to have the same behaviour (no dispersion). The battery electro-thermal model is simplified. The battery is described as an equivalent large cell. The configuration of the battery is 96 cells in series and two branches in parallel. The battery electro-thermal model is derived from [9] and is presented in Fig. 8. The parameters are the following:

- the Open Circuit Voltage (OCV_{Bat}),
- the Equivalent Series Resistance (ESR_{Bat}),
- the thermal capacitance of the battery (C_{ThBat}),
- the thermal resistance of the battery (R_{ThBat}).

Table 2 gives the values of the battery parameters. The battery electro-thermal model is organized with EMR.

As a consequence, the model is organized with power variables and the integral causality is compulsory. Equations of a battery electro-thermal model have been developed in [9].

Table 2 Parameters of the battery electro-thermal model [36]

Parameter	Name	Value	Unit
Battery config. (n_{SCells} series x n_{PCells} parallel)	n_{SCells} x n_{PCells}	96 x 2	cells
Battery nominal voltage	u_{BatNom}	345.6	V
Battery capacity	C_{AhBat}	126	Ah
Battery ESR (@ 25°C, 50% SoC)	ESR_{Bat}	78.2	mΩ
Battery mass	m_{Bat}	305	kg
Battery thermal resistance	R_{ThBat}	23.0	$mK.W^{-1}$
Battery thermal capacitance	C_{ThBat}	202	$kJ.K^{-1}$

The SoC and OCV_{Bat} equations are expressed in a classical way.

$$SoC(\%) = SoC_{Init} - \frac{100}{3600.C_{AhBat}}.\int_0^t i_{Bat}\,dt \quad (10)$$

$$OCV_{Bat} - ESR_{Bat}\cdot i_{Bat} = u_{Bat} \quad (11)$$

For EMR, the variables must be power variables (flow and effort). In the thermal domain, the flow variable is the entropy flow (q_S in W/K) and the power variable is the temperature (T in K). The heating power P is the product of those two variables.

$$P = q_S.T \quad (12)$$

The electro-thermal battery model presented in fig. 4 is simplified. The endo/exo-thermic effects [37] are neglected in our battery model. The heating power is considered to come only from Joule effect.

$$q_{S1} = \frac{ESR_{Bat}\, i_{Bat}^2}{T_{Bat}} \quad (13)$$

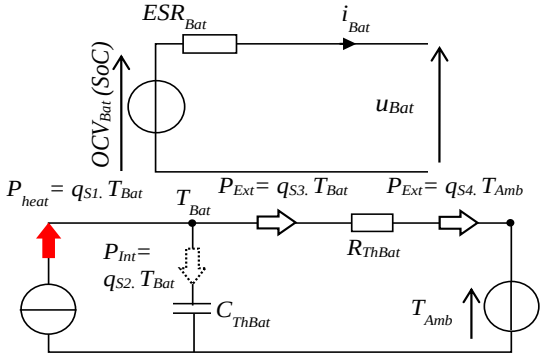

Fig. 8 Structure of the simplified electro-thermal model

The classical differential equation (14) used for the evolution of the temperature is re-organized in an integral form. This is to meet the integral causality (compulsory in EMR), as shown in (16). $T_{BatInit}$ is the initial temperature inside the battery.

$$\frac{dT_{Bat}}{dt} = \frac{P_{Int}}{C_{ThBat}} \tag{14}$$

$$\text{with } P_{Int} = (q_{S1} - q_{S3}).T_{Bat} \tag{15}$$

$$\Leftrightarrow T_{Bat} = T_{BatInit}.e^{\frac{1}{C_{ThBat}}\int_0^t (q_{S1}-q_{S3})dt} \tag{16}$$

The equations associated with the thermal resistance calculate the entropy flows q_{S3} and q_{S4}. T_{Amb} is the ambient air temperature.

$$q_{S3} = \frac{T_{Bat} - T_{Amb}}{(R_{ThBat}).T_{Bat}} \tag{17}$$

$$q_{S4} = \frac{T_{Bat} - T_{Amb}}{(R_{ThBat}).T_{Amb}} \tag{18}$$

Fig. 9 shows the EMR of the presented electro-thermal model of the Renault Zoe battery. Then, the simulated temperature is compared with the battery temperature measured inside a Zoe for a 22 kW charger during 1h (Fig. 10). The experimental temperature is recorded through 12 sensors placed by the manufacturer inside the battery of the Renault Zoe during charging. The results are presented with the average and extreme values of the 12 temperatures measured. At each moment of the test, there is a +/- 1°C dispersion. This dispersion seems to be related with sensors offsets, as it is present since the beginning of the test (the car was at total rest for 5 hours before the test). As a consequence, an average thermal model is justified for the study of the Renault Zoe battery. The average error of the model with the battery temperature is 0.25 °C. When normalized with the temperature variation during the test (+ 5.34 °C), it gives a relative error of 4.7 %.

A comparison was also made for the electrical part. The model battery voltage has been compared with experimental measurements in the Renault Zoe (Fig 11). The mean relative error on the battery voltage is lower than 1 %.

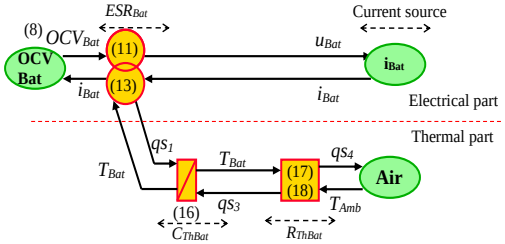

Fig. 9 EMR of the battery electro-thermal model

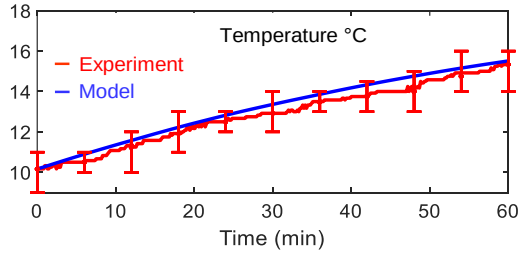

Fig. 10 Zoe battery temperature evolution during a 22 kW charging

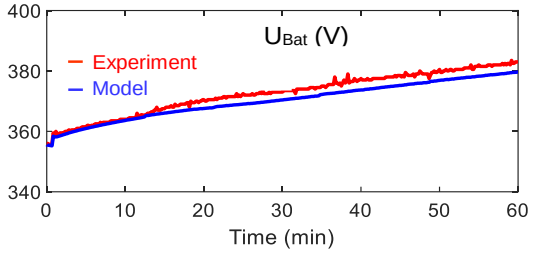

Fig. 11 Comparison of model and experiment for u_{Bat}

F. Vehicle traction, charger and parking model

The traction model has been developed, organized with EMR and validated in [38] for the Renault Zoe. The parameters of the model are given in Table 3.

Table 3 Parameters of the studied EV [39]

Parameter	Name	Value	Unit
Aerodynamic drag coefficient	c_X	0.333	---
Front surface	S	2.25	m²
Vehicle mass+ 2 passengers	M_{Tot}	1600	kg
Air volumic mass	φ_{Air}	1.3	kg/m³
Road friction	f_0	220	N
Wheel radius	r_{Wheel}	0.30	M
Gearbox coefficient	k_{Gear}	9.34	---
Traction efficiency	η_{Tract}	0.86	---

To simplify the traction presentation, the electric drive (machine, control and power electronics) is grouped with the gearbox and the wheels. In EMR it is represented as a multi-physical (electro-mechanical) energy conversion element with a fixed power efficiency (η_{Tract}^{k}). The value of k depends on the power direction.

$$\begin{cases} i_{Drive} = \eta_{Tract}^{k} \dfrac{V_{EV}\, f_{Wheel}}{u_{Bat}} \\ f_{Wheel} = f_{WheelRef} \end{cases} \tag{19}$$

k=1 if traction mode
k=-1 if regenerative braking

where i_{Drive}, V_{EV}, U_{Bat} and f_{Wheel} are the drive current, the vehicle velocity, the battery voltage and the wheel force.
The brake and the traction force of the wheels are coupled together on the wheels. f_{Tot} is the total force due to traction and braking.

$$f_{Tot} = f_{Wheels} - f_{Brake} \tag{20}$$

The chassis is an energy accumulation element. It is expressed with the integral causality.

$$v_{EV} = \frac{1}{M_{Tot}} \int_0^t f_{Tot} - f_{Res} dt \tag{21}$$

The road is a source of resistive forces. Resistive forces (f_{Res}) are composed of the road friction f_0 and the aerodynamical forces. Slope is not considered here, as we study normalized cycles, but it can be added easily.

$$f_{Res} = f_0 + \frac{1}{2} c_x S \varphi_{Air} {v_{EV}}^2 \tag{22}$$

In order to study a driving scenario in the following parts, a driving cycle should be used. As a consequence, the reference speed as a function of time is the input of the vehicle simulation (v_{VehRef}). With EMR, the control structure is deduced by mirror effect. For all control variables, Ref refers to a reference value.

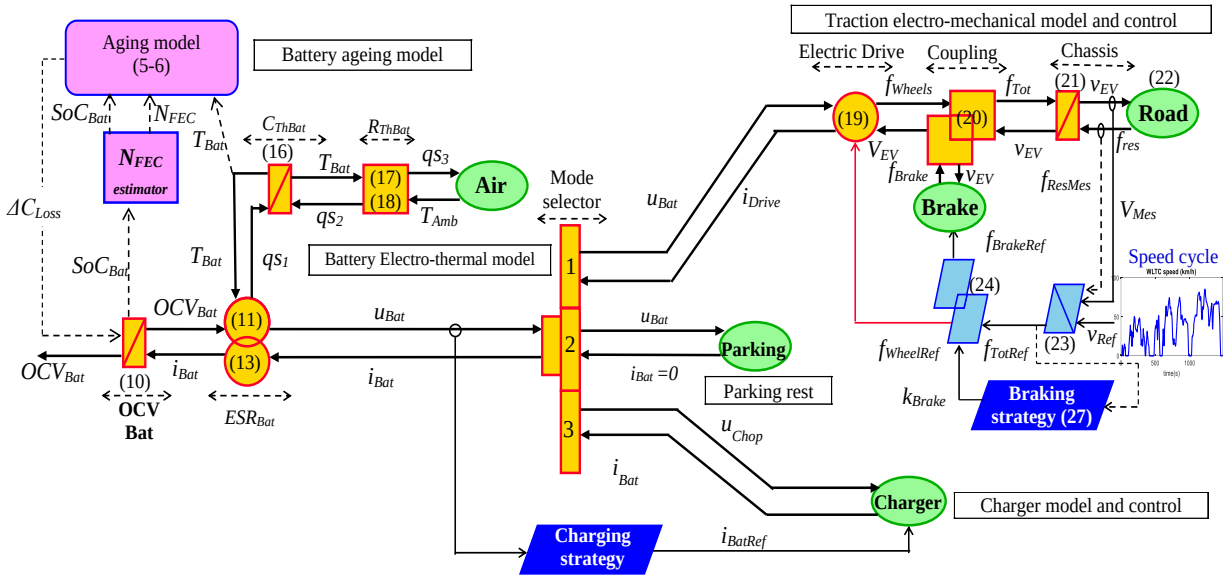

Fig. 12 Implementation of the full EV model by using EMR

As the chassis presents a delay in (21) (integral), a controller ($C(s)$) should be used.

$$f_{TotRef} = f_{ResMes} + C(s).(v_{Ref} - v_{Mes}) \quad (23)$$

The coupling is inverted with a distribution element.

$$\begin{cases} f_{wheelsRef} = k_{Brake}.f_{TotRef} \\ f_{BrakeRef} = (1 - k_{Brake}).f_{TotRef} \end{cases} \quad (24)$$

The braking strategy generates a factor k_{Brake} which distributes the wheel force between electrical (traction/brake) and mechanical brake (24). When braking is activated, 60% of the braking is electrical.

$$\begin{cases} k_{Brake} = 1 \; if \; f_{TotRef} > 0 \; (traction \; mode) \\ k_{Brake} = 0.6 \; if \; f_{TotRef} \leq 0 \; (braking \; mode) \end{cases} \quad (25)$$

Although this EV traction model is simplified, the average error with experimental results of battery current is 2% [38] .

The mode selector is a switching EMR element and allows to choose if the vehicle is in charging, driving or parking mode.

The charger is represented here by an equivalent source driven by a Constant Current, Constant Voltage strategy (CC-CV). A detailed presentation of the charger has been developed in [40].

The parking phase is represented by an equivalent current source with a current of 0 A.

III. Impact of the Charging Time Interval on the Battery Aging for Various Usages

A. Integration of the full model

EMR is used as a unique representation for every sub-system. The sub-systems are easily interconnected by using this graphical description (Fig. 12) to form the system model. The battery current comes from the vehicle traction subsystem or the charger. The actual battery capacity is updated at every aging model time step with the evolution of the *SoH*. A WLTC (Worldwide Harmonized Light Vehicles Test Cycle) class 3 is used as an input for the driving phases (Fig. 13.a). It is a driving cycle with urban, sub-urban and motorway parts. The total distance is 23 km. Two WLTC cycles are considered to be achieved every day (this corresponds to 17 000 km per year). In Fig 13, the battery voltage (b), current (c), temperature (d), SoC (e) and capacity loss (f) are also represented. The self-heating is moderate because of the short trip. All the charges are performed at a current level (C/6) corresponding to a 6.7 kW AC charging [20]. The ambient air temperature for all simulations is 20°C.

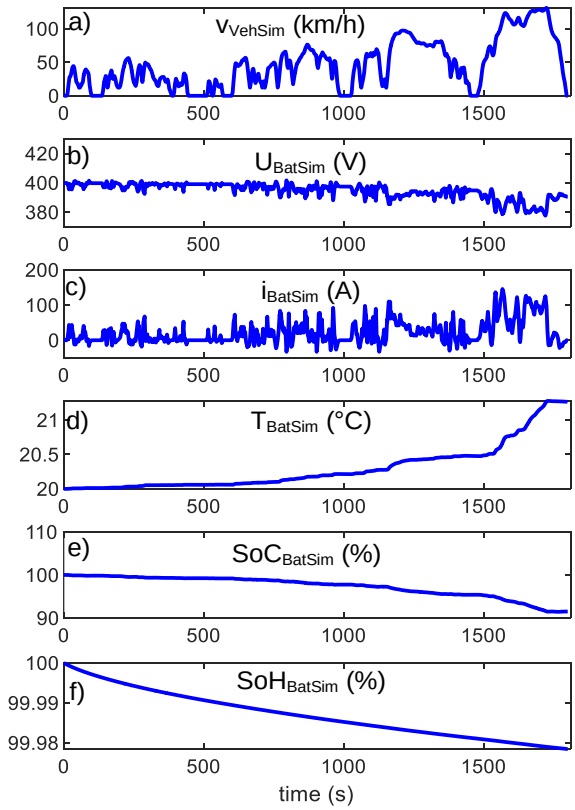

Fig. 13 WLTC driving cycle a) battery simulated voltage b), current c), temperature d), SoC e), and SoH evolution f)

Combining the vehicle model with the aging model also results in a multiple time scale system. The vehicle subsystem has much faster dynamics (hundreds of milliseconds) than the aging subsystem (several years). The difficulty to simulate such problems is that the subsystems are coupled and depend on each other with different time scales. Therefore, it can penalize the computational time.

It is possible to simulate the aging model with the same time step as the traction and battery electro-thermal one. However, the aging part makes the global simulation 10 times longer than when a unique time step is applied throughout the model. This is a problem when 10 years of operation are simulated for the aging study. In this paper, the multi-step method [41] is performed to tackle this problem. It is implemented on MATLAB Simulink. The system is split into several slow and fast subsystems [42], allowing to use adapted step times. The time step chosen for the simulation of the fast dynamics is 10 ms and 100 s for the battery aging model.

B. *Everyday charging scenarios (fixed interval) for 10 years*

In this part, different charging scenarios are studied. They are presented in Fig. 14 for one week.

S1 to S3 correspond to scenarios where the battery of the vehicle is charged every day. The difference is the initial SoC (respectively 100 %, 60 % and 30 %) computed with the degraded capacity. The scenarios are simulated for 10 years to estimate the evolution of the SoH.

First, the everyday charging scenarios are tested (Fig. 15). Depending on the SoC interval, aging can be very different. As a matter of fact, after 10 years the degradation can go from 15 % (S3) to 28 % (S1), which represents a multiple of 1.9, for the same driving distance.

A close look at Fig. 14 shows that higher the SoC is, faster is the aging. A way to slow down battery aging would be to stay at low SoC (S3 for example). Nevertheless, the charging stations usually recharge the batteries of the vehicles to full SoC level. The user could stop the recharge before the end but it is not practical. In the next section, longer intervals for recharge are studied in order to lower the SoC in a more practical way.

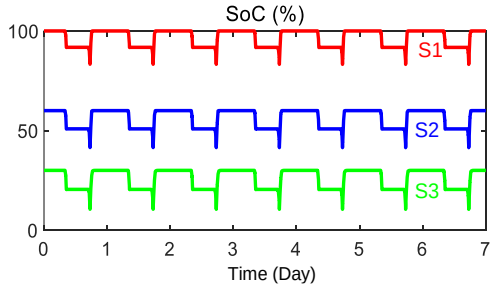

Fig. 14 Battery SoC evolution for every day charge scenarios

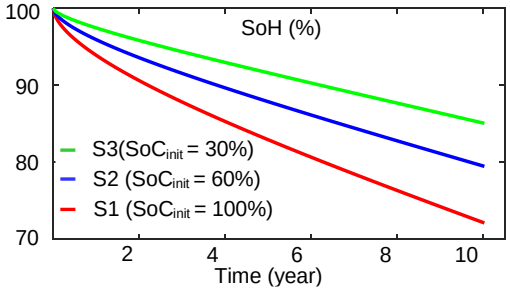

Fig. 15 SoH evolution for everyday charges

C. *Various charging intervals scenarios for 10 years*

In this section the initial SoC is fixed at 100 %. The variable under consideration is the time interval between charges. For example, a charge can be made every 2 days (S4) or every 4 days (S5). With longer intervals between charges, the average SoC level is lower because the SoC decreases for a longer period than when the EV is charged every day.

The S4 and S5 scenarios are simulated for 10 years. The scenario S1 (everyday recharge) is also simulated for comparison.

Simulation results in Fig. 17 show that charging every 4 days reduces the aging at 10 years by 19 % compared to charging every day. The difference between charging every day and every two days is less obvious (5.7 % aging reduction). These tendencies are also observed at the end of the first year (Fig. 18). It can be noticed that the evolution of the SoC during S1 (Fig. 14) is close to S4 (Fig. 16), whereas for S5, the SoC is decreasing far below. Having a longer interval between two charges implies a lower mean SoC level and thus a slower aging.

D. *Synthesis for reaching 80% SoH*

A synthesis has been performed to identify the main impacting factor on aging. In this study, as described before, the daily driving distance of the EV is fixed. The variable for the scenarios is the SoC variation between charge. The average SoC has been chosen to represent every scenario. In Fig. 19 the time to reach 80% SoH has been represented as a function of the average SoC for every scenario. This is a common value recommended by the manufacturers although the batteries can operate at further degradation [21]. S3 has been simulated for 14 years to reach this value.

A clear trend is extracted with a decrease of time to reach 80% SoH when the average SoC is increasing.

This is a direct consequence of the SoC dependence in the aging law presented in (1). Cumulated variations under aging law allows to estimate the time to reach 80% capacity for each scenario. This time goes from 6.3 years to 14 years under different simulation conditions. The 4 days recharge scenario (S5) takes 8.6 years (144 10^3 km) compared to the (S1) daily charging 6.3 years (107 10^3 km). This means a 36 % of time extension to reach 80% for *SoH*.

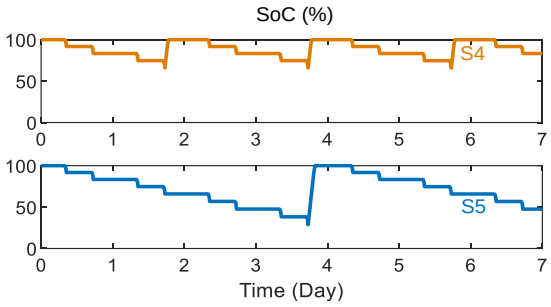

Fig. 16 Battery SoC evolution for different charging intervals

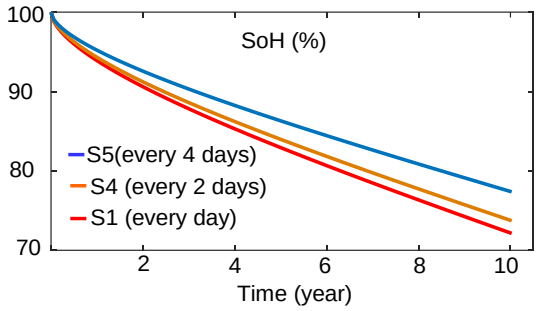

Fig. 17 SoH evolution for different charging intervals

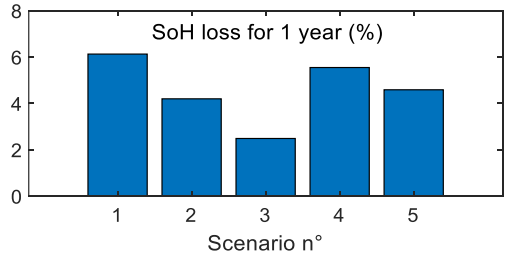

Fig. 18 Capacity degradation after one year of use

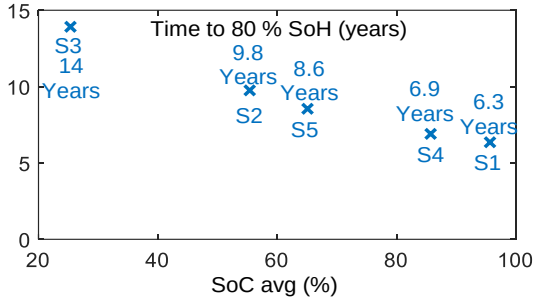

Fig. 19 Time to reach 80% for capacity vs average SoC

E. Extension to US06 cycle

Another type of cycle is used in this study (US06). It is mainly a motorway cycle. The cumulated distance is 12 km. Fig. 20 shows the velocity, the evolution of the temperature and the SoC over time. The self-heating is low and the evolution of the SoC is slightly lower than for the WLTC (-6.5% instead of 9%). The same scenarios are studied. Fig. 21 presents the aging results. They are similar to the WLTC one (the lower amount of FEC is compensated by the higher SoC as a function of time). The same tendencies are observed.

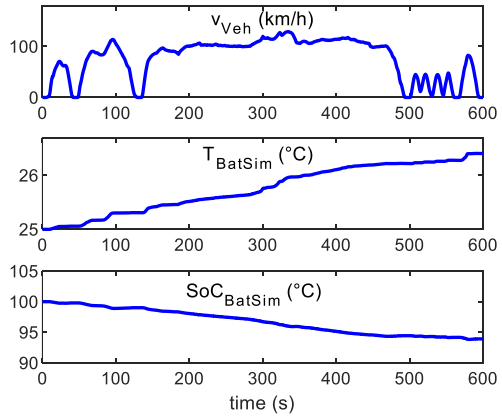

Fig. 20 US 06 simplified presentation

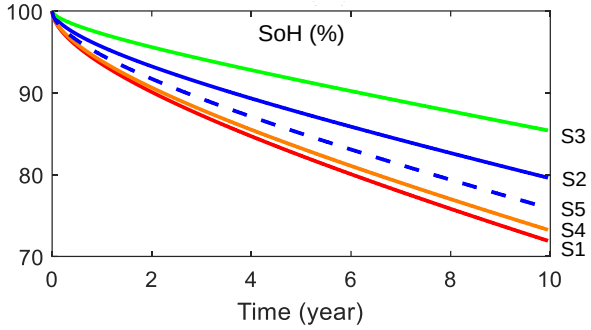

Fig. 21 SoH evolution for a US06 cycle

IV. Conclusion

In this paper, a new model for battery aging has been proposed. It is based on the effect of temperature, SoC and the amount of full equivalent cycles (FEC). Aging is a dynamical phenomenon with causality (present state depends on past events). Therefore, an approach based on differential (infinitesimal variations) is used in this paper.

The parameters of the proposed aging law are identified using aging results from the literature corresponding to the cells used in the 41 kWh Renault Zoe. The model has been validated with a separate cycling aging result not used for identification. The results obtained with the model are compared with experimental results and show an average relative error of 2.24 % on the SoH value.

The aging model has been identified for mild to hot battery temperatures. As a consequence, this model is not adapted for cold temperatures.

An electro-thermal model of the battery is used to reproduce the evolution of the battery temperature. It has been validated with experimental results (measured on a real car) with an average absolute value of 0.25 °C and an average relative value of 4.7% normalized with the total variation.

The aging and the electro-thermal models have been coupled with a vehicle traction model validated in another publication.

The complete simulation model (including driving, parking and charging) is used to study the impact of charging intervals on battery aging for a Renault Zoe. For the same driving use (2 WLTC per day) and the same low current level for recharge, different SoC scenarios are investigated. The effect on the SoH degradation are compared over 10 years. Simulation results show that keeping average SoC value as low as possible is the key to improve the battery lifespan. This trend is evident after one year. Another cycle (US06) is used for confirmation.

From the user point of view, it means performing charges with longer time interval and charging the battery when it is nearly discharged. In practice, for the same daily driving distance, a charge every 4 days increased the time to reach 80% SoH by 36 % compared to a daily charge.

Other cells, vehicles can be studied with this method. The only point to change is to define the new battery model with results corresponding to the cells used in this battery. Using larger battery ageing databases for model identification is of interest for future works for accuracy and generalization purposes.

V. Acknowledgement

This work is a part of the CUMIN program (Campus of University with Mobility based on Innovation and carbon Neutral) of the University of Lille.
These researches are performed under the framework of the MEGEVH network (French network on hybrid and electric vehicles).
This work has been achieved within the framework of EE4.0 (Energie Electrique 4.0) project. EE4.0 is co-financed by European Union with the financial support of the European Regional Development Fund (ERDF), French State and the French Region of Hauts-de-France

VI. Bibliography

[1] W. Kim, P. -Y. Lee, J. Kim and K. -S. Kim, "A Robust State of Charge Estimation Approach Based on Nonlinear Battery Cell Model for Lithium-Ion Batteries in Electric Vehicles," *IEEE Transactions on Vehicular Technology*, vol. 70, no. 6, pp. 5638-5647, June 2021, doi: 10.1109/TVT.2021.3079934.

[2] C. C. Chan, A. Bouscayrol, K. Chen, "Electric, Hybrid and Fuel Cell Vehicles: Architectures and Modeling", *IEEE transactions on Vehicular Technology*, vol. 59, no. 2, pp. 589-598, February 2010, DOI: 10.1109/TVT.2009.2033605.

[3] International Energy Agency, "Global EV Outlook 2022," 2022

[4] J. Zhang, M. Salman, W. Zanardelli, S. Ballal and B. Cao, "An Integrated Fault Isolation and Prognosis Method for Electric Drive Systems of Battery Electric Vehicles," in *IEEE Transactions on Transportation Electrification*, vol. 7, no. 1, pp. 317-328, March 2021, doi: 10.1109/TTE.2020.3025107.

[5] J. F. Peters, M. Baumann, B. Zimmermann, J. Braun, M. Weil, "The environmental impact of Li-Ion batteries and the role of key parameters – A review," *Renewable and Sustainable Energy Reviews*, Vol. 67, 2017, pp. 491-506, doi.org/10.1016/j.rser.2016.08.039.

[6] "How clean are electric cars?", transportenvironment.org, https://www.transportenvironment.org/discover/how-clean-are-electric-cars/, (accessed Apr. 17, 2023).

[7] M. V. Morganti, S. Longo, M. Tirovic, C. -Y. Blaise and G. Forostovsky, "Multi-Scale, Electro-Thermal Model of NMC Battery Cell," IEEE *Transactions on Vehicular Technology*, vol. 68, no. 11, pp. 10594-10606, Nov. 2019, doi: 10.1109/TVT.2019.2943052.

[8] V. Chamola, A. Sancheti, S. Chakravarty, N. Kumar and M. Guizani, "An IoT and Edge Computing Based Framework for Charge Scheduling and EV Selection in V2G Systems," *IEEE Transactions on Vehicular Technology*, vol. 69, no. 10, pp. 10569-10580, Oct. 2020, doi: 10.1109/TVT.2020.3013198.

[9] R. German, S. Shili, A. Desreveaux, A. Sari, P. Venet and A. Bouscayrol, "Dynamical Coupling of a Battery Electro-Thermal Model and the Traction Model of an EV for Driving Range Simulation," *IEEE Transactions on Vehicular Technology*, vol. 69, no. 1, pp. 328-337, Jan. 2020, doi: 10.1109/TVT.2019.2955856.

[10] M. Ben-Marzouk, S. Pelissier, G. Clerc, A. Sari and P. Venet, "Generation of a Real-Life Battery Usage Pattern for Electrical Vehicle Application and Aging Comparison With the WLTC Profile," *IEEE Transactions on Vehicular Technology*, vol. 70, no. 6, pp. 5618-5627, June 2021, doi: 10.1109/TVT.2021.3077671.

[11] A. Alyakhni, L. Boulon, J. -M. Vinassa and O. Briat, "A Comprehensive Review on Energy Management Strategies for Electric Vehicles Considering Degradation Using Aging Models," in IEEE Access, vol. 9, pp. 143922-143940, 2021, doi: 10.1109/ACCESS.2021.3120563

[12]] P. Ramadass, B. Haran, P. M. Gomadam, R. White, and B. N. Popov,''Development of first principles capacity fade model for Li-ion cells,''J. Electrochim. Soc., vol. 151, no. 2, 2004, Art. no. A196, doi:10.1149/1.1634273.

[13] Y. Xing, E.W.M. Ma, K.-L. Tsui, M. Pecht, "An ensemble model for predicting the remaining useful performance of lithium-ion batteries," Microelectronics Reliability, Volume 53, Issue 6, 2013, Pages 811-820, ISSN 0026-2714, https://doi.org/10.1016/j.microrel.2012.12.003.

[14] T.D Patil, E. Vinot, S. Ehrenberger, R. Trigui, E. Redondo-Iglesias, "Sensitivity Analysis of Battery Aging for Model-Based PHEV Use Scenarios". *Energies* vol. 16, no. 4, pp. 1749, , Feb. 2023, https://doi.org/10.3390/en16041749.

[15] M. Abdel-Monem, K. Trad, N. Omar, O. Hegazy, P. Van den Bossche, and J. Van Mierlo, "Influence analysis of static and dynamic fast-charging current profiles on ageing performance of commercial lithium-ion batteries," *Energy*, vol. 120, pp. 179–191, Feb. 2017, doi: 10.1016/j.energy.2016.12.110.

[16] E. H. El Brouji, O. Briat, J. -M. Vinassa, N. Bertrand and E. Woirgard, "Impact of Calendar Life and Cycling Ageing on Supercapacitor Performance," in IEEE Transactions on Vehicular Technology, vol. 58, no. 8, pp. 3917-3929, Oct. 2009, doi: 10.1109/TVT.2009.2028431.

[17] X. Hu, Y. Zheng, X. Lin, and Y. Xie, "Optimal Multistage Charging of NCA/Graphite Lithium-Ion Batteries Based on Electrothermal-Aging Dynamics," *IEEE Trans. Transportation Electrification.*, vol. 6, no. 2, pp. 427–438, Jun. 2020, doi: 10.1109/TTE.2020.2977092.

[18] I.J. Fernández, C.F. Calvillo, A. Sánchez-Miralles, J. Boal,"Capacity fade and aging models for electric batteries and optimal charging strategy for electric vehicles," *Energy*, Vol. 60, 2013, pp. 35-43, https://doi.org/10.1016/j.energy.2013.07.068.

[19] A. Houbbadi, R. Trigui, S. Pelissier, E. Redondo-Iglesias, and T. Bouton, "Optimal Scheduling to Manage an Electric Bus Fleet Overnight Charging," *Energies*, vol. 12, no. 14, p. 2727, Jul. 2019, doi: 10.3390/en12142727.

[20] M. Senol, I. Safak Bayram, Y. Naderi and S. Galloway, "Electric Vehicles under Low Temperatures: A Review on Battery Performance, Charging Needs, and Power Grid Impacts," *IEEE Access*, early access, Apr. 2023, doi: 10.1109/ACCESS.2023.3268615.

[21] E. Redondo-Iglesias, P. Venet, S. Pelissier, "Calendar and cycling ageing combination of batteries in electric vehicles," *Microelectronics Reliability*, Vol.s 88–90, 2018, pp. 1212-1215, https://doi.org/10.1016/j.microrel.2018.06.113.

[22] S. Grolleau, A. Delaille, and H. Gualous, "Predicting lithium-ion battery degradation for efficient," *EVS27* Barcelona, Spain, November 2013.

[23] M. Schimpe, M. E. von Kuepach, M. Naumann, H. C. Hesse, K. Smith, and A. Jossen, "Comprehensive Modeling of Temperature-Dependent Degradation Mechanisms in Lithium Iron Phosphate Batteries," 2018 J. Electrochem. Soc. 165 A181, DOI 10.1149/2.1181714jes.

[24] T. Mesbahi, N. Rizoug, P. Bartholomeüs, R. Sadoun, F. Khenfri and P. Le Moigne, "Dynamic Model of Li-Ion Batteries Incorporating Electrothermal and Ageing Aspects for Electric Vehicle Applications," in IEEE Transactions on Industrial Electronics, vol. 65, no. 2, pp. 1298-1305, Feb. 2018, doi: 10.1109/TIE.2017.2714118.

[25] G. Suri, S. Onori, "A control-oriented cycle-life model for hybrid electric vehicle lithium-ion batteries," Energy, Volume 96, 2016, Pages 644-653, ISSN 0360-5442, https://doi.org/10.1016/j.energy.2015.11.075.

[26] A. Bouscayrol, J. P. Hautier, B. Lemaire-Semail, "Graphic Formalisms for the Control of Multi-Physical Energetic Systems", Systemic Design Methodologies for Electrical Energy, tome 1, Analysis, Synthesis and Management, Chapter 3, ISTE Willey editions, October 2012, ISBN: 9781848213883.

[27] E. Martinez-Laserna, I. Gandiaga, E. Sarasketa-Zabala, J. Badeda, D.-I. Stroe, M. Swierczynski, A. Goikoetxea, "Battery second life: Hype, hope or reality? A critical review of the state of the art," Renewable and Sustainable Energy Reviews, Volume 93, Pages 701-718, 2018, https://doi.org/10.1016/j.rser.2018.04.035.

[28] J. Neubauer, A. Pesaran, "The ability of battery second use strategies to impact plug-in electric vehicle prices and serve utility energy storage applications, Journal of Power Sources, Volume 196, Issue 23, pp. 10351-10358, 2011, https://doi.org/10.1016/j.jpowsour.2011.06.053.

[29] M. Arrinda et al., "Application Dependent End-of-Life Threshold Definition Methodology for Batteries in Electric Vehicles," Batteries, vol. 7, no. 1, p. 12, Feb. 2021, doi: 10.3390/batteries7010012.

[30] C.R. Birkl, M. R. Roberts, E. McTurk, P. G. Bruce and D. A. Howey, "Degradation diagnostics for lithium ion cells", *Journal of Power Sources*, vol. 341, pp. 373-386, 10.1016/j.jpowsour.2016.12.011, Feb. 2017, https://linkinghub.elsevier.com/retrieve/pii/S0378775316316998.

[31] S. Grolleau et al., "Calendar aging of commercial graphite/LiFePO4 cell e Predicting capacity fade under time dependent storage conditions," *Journal of Power Sources*, vol. 255, pp. 450-458, 2014.

[32] J. Wang, J. Purewal, and M. W. Verbrugge, "Degradation of lithium ion batteries employing graphite negatives and nickel–cobalt–manganese oxide + spinel manganese oxide positives: Part 1, aging mechanisms and life estimation," *Jounal of Power Sources*, vol. 269, pp. 937-948, 2014.

[33] "LG Chem, Rechargeable Lithium Ion Battery E63 : product specifications," https://xebike.com/wp-content/uploads/2019/12/lg-e63datasheet.pdf, (accessed Apr. 17, 2023).

[34] E. Redondo-Iglesias, P. Venet and S. Pelissier, "Modelling Lithium-Ion Battery Ageing in Electric Vehicle Applications—Calendar and Cycling Ageing Combination Effects", Batteries, vol 6, n° 1, pp. 14, Fev. 2020, doi: 10.3390/batteries6010014.

[35] Maher K, Yazami R (2014) A study of lithium ion batteries cycle aging by thermodynamics techniques. Journal of Power Sources 247:527–533. https://doi.org/10.1016/j.jpowsour.2013.08.053.

[36] D. Phetsinorath, Sahar Khaleghi, John Klein, Maxence Giraud, Marius Ciocan "Multi-level behaviour models of batteries," PANDA H2020 GA# 824256, D 2.3 confidential report, July 2020.

[37] N. Damay, C. Forgez, M.P. Bichat, G. Friedrich, "A method for the fast estimation of a battery entropy-variation high-resolution curve – Application on a commercial LiFePO4/graphite cell", *Journal of Power Sources*, Vol. 332, 2016, pp. 149-153, , https://doi.org/10.1016/j.jpowsour.2016.09.083.

[38] A. Desreveaux, E. Hittinger, A. Bouscayrol, E. Castex and G. M. Sirbu, "Techno-Economic Comparison of Total Cost of Ownership of Electric and Diesel Vehicles," *IEEE Access*, vol. 8, pp. 195752-195762, 2020, doi: 10.1109/ACCESS.2020.3033500.

[39] G. Sirbu, A. Desrevaux, C. Hussar, N. Boicea, "Report on the virtual testing of the BEV", PANDA H2020 GA# 824256, D4.3 Deliverable, public report, January 2022, [Online] available: https://project-panda.eu/ Accessed January 2022.

[40] R. German, P. Delarue and A. Bouscayrol, "Battery pack self-heating during the charging process," 2018 IEEE International Conference on Industrial Technology (ICIT), Lyon, France, 2018, pp. 2049-2054, doi: 10.1109/ICIT.2018.8352504.

[41] M. Crow and M. Ilic, "The parallel implementation of the waveform relaxation method for transient stability simulations," *IEEE Transactions on, Power Systems*, vol. 5, no. 3, pp. 922–932, 1990.

[42] M. Crow and J. Chen, "The multirate simulation of facts devices in power system dynamics," *IEEE Transactions on Power Systems*, vol. 11, no. 1, pp. 376–382, 1996.

Alla Ndiaye obtained his master in electrical engineering in 2020 at the university of Lille. Since 2020 he is a PhD student in Electrical system Engineering at the University of Lille/France. His current research topics include electric vehicle charging and battery aging.

Ronan German was born in Roanne, France, in 1986. He received the master degree in electrical engineering at national institute of applied sciences of Lyon, France in 2009. From 2010 to 2013 he was a Ph.D. student from Lyon1 university under a joint supervision with Bordeaux1 University. From 2013 to 2015 he made two years as an assistant professor at the University of Lyon. Since September 2015 he became an associate professor at the university of Lille in the Laboratory of Electrical Engineering and Power electronics (L2EP). His current research interests include management of energy storage systems in the context of electric vehicles as a function of various parameters.

Alain Bouscayrol received a Ph.D. degree in Electrical Engineering from the Institut National Polytechnique de Toulouse, France, in 1995.

From 1996 to 2005, he was Associate Professor at University of Lille, France, where he has been a Professor since 2005. From 2004 to 2019, he managed the national network on Energy Management of Hybrid Electric Vehicles France. Since 2016, he has coordinated the interdisciplinary program CUMIN on electromobility for campus of universities. He has initiated the Energetic Macroscopic Representation (EMR) graphical formalism in 2000 for the description and the control of energy conversion systems. His research interests include graphical descriptions for control of electric drives, railway traction systems, electrified vehicles and hardware-in-the-loop testing.

Margot Gaetani-Liseo is an Assistant Professor at Lyon 1 University since 2022, where she develops his research activities at the AMPERE Laboratory. She received a Ph.D. degree in Electrical Engineering from the Toulouse University (Paul Sabatier - Toulouse 3) in 2021 with the Laboratory of Systems Analysis and Architecture (LAAS-CNRS). His current research work focuses on the Energy Storage System (ESS) - mostly lead acid and lithium-ions batteries - behaviour, control and optimal design (sizing/management) in electrical vehicles and microgrids or grids applications. She works both on ESS modelling and characterization at different scales, from individual cell to an overall system approach in order to develops optimized Battery Management System (BMS) and Energy Management System (EMS).

Pascal Venet received the Ph.D. degree in electrical engineering in 1993 from the Lyon 1 University, France. After postdoctoral positions, he joined the Lyon 1 University as Assistant Professor from 1995 to 2009. Since 2009, he has been Professor of Electrical Engineering at the Lyon 1 University.
He has developed his research activity within an Electrical Engineering Laboratory (AMPERE). He is co-leader of "Safe Systems and Energies" research team within the laboratory.
His current research interests include characterization, modelling, fault diagnostics, reliability and ageing of energy storage systems (such as batteries, supercapacitors and capacitors). He also studies the Battery Management System (BMS) including cell balancing of cells, determination of state of charge and state of health of battery.

Elodie Castex is currently a Full Professor with the Geography and Urban Planning Department, University of Lille, Lille, France. She conducts research on transportation planning and mobility analysis at the laboratory TVES (Territoires, Villes, Environnement & Société, EA 4477) especially on the subject of news services in mobility and electromobility systems (electrics vehicles, car sharing, carpooling, demand responsive transportation, etc).

Appendix A: EMR Pictograms

	Source element (energy source)	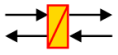	Accumulation element (energy storage)	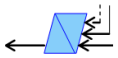	Indirect inversion (closed-loop control)
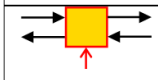	Mono-physical conversion element	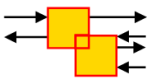	Mono-physical coupling element (energy distribution)	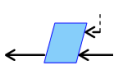	Direct inversion (open-loop control)
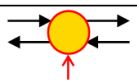	Multi-physical conversion element	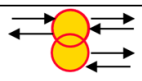	Multi-physical coupling element (energy distribution)	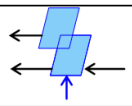	Coupling inversion (energy criteria)